doi.org/10.36721/PJPS.2024.37.6.REG.1213-1222.1

Atractylenolide I regulates colorectal cancer cells' biological processes and glycolysis via KRT7

Yutao Xie[1,2], Yunlong Wang[1,2], Lin Chen[1,2], Junshan Long[1,2], Ruyong Zhu[3] and Huihui Zheng[4]*

[1]Beijing Anzhen Nanchong Hospital, Capital Medical University & Nanchong Central Hospital
[2]Nanchong Key Laboratory of Individualized Drug Therapy
[3]Chongqing Hospital of Traditional Chinese Medicine Preparation Center
[4]Pharmacy Department of Chong Qing Bishan District TCM Hospital

Abstract: Atractylenolide I (ATL-I) can interfere with Colorectal cancer (CRC) cell proliferation by changing apoptosis, glucose metabolism, and other behaviors, making it an effective drug for inhibiting CRC tumor growth. In this paper, we investigated the interactions between ATL-I and Keratin 7 (KRT7), a CRC-specific marker, to determine the potential pathways by which ATL-I inhibits CRC development. The KRT7 expression level in CRC was predicted online using the GEPIA website and then validated. HCT-116 cells' proliferation and invasion ability were determined using MTT and Transwell assays and the apoptosis rate using flow cytometry. Glucose consumption, lactate and ATP production levels were measured in HCT-116 cells using appropriate kits. Created the subcutaneous graft tumor model and identified the ATL-I effect *in vivo*. KRT7 was highly increased in CRC cells, KRT7 knockdown and overexpression prevented and encouraged malignant biological processes, as well as glycolysis. ATL-I acts by inhibiting the expression of KRT7, which can greatly inhibit the formation of CRC transplantation tumors in nude mice. ATL-I can impede the malignant biological process and glycolysis of CRC cells by inhibiting KRT7 expression *in vitro* and *in vivo*.

Keywords: Atractylenolide I, Keratin 7, colorectal cancer, glycolysis.

Submitted on 19-08-2024 – Revised on 02-10-2024 – Accepted on 16-10-2024

INTRODUCTION

Colorectal cancer (CRC) is one of the most common forms of gastrointestinal malignancies worldwide, with China accounting for 28.8% of new cases and 30.6% of fatalities worldwide (Sung *et al.* 2021). Conventional therapies include surgery, chemotherapy, radiation and targeted therapy. Although surgery and chemotherapy have long been the initial lines of treatment for CRC patients, complications such as postoperative complications, resistance to chemotherapy, toxic and side effects of drugs and high rates of metastasis and recurrence contribute to a poor prognosis (El-Shami *et al.,* 2015; Pachman *et al.,* 2015). Targeted therapy is a new strategy that has been beneficial in increasing the overall survival rate of CRC patients; nevertheless, its medications are pricey, resistant, and not appropriate for all patients (Aldea *et al.,* 2021; Paleari 2022). Herbal medicines, which are typically less expensive, mostly natural and contain numerous similar compounds, have the advantages of being multi-targeted, with less side effects, and very effective and have a long history of usage in the research of CRC and other malignancies (Chen *et al.,* 2023). In recent years, Chinese medicinal preparations have made some progress in CRC therapy, For example, Curcumin is anti-proliferation, anti-angiogenesis, and anti-metastasis in CRC cells (Calibasi-Kocal *et al.,* 2019); Berberine, an extract of Rhizoma Coptidis, significantly improved the progression of CRC tumours in mice (Wang *et al.,* 2018); Geraniin interfered with the proliferation of HTC116 in CRC cells and induced mitotic aberrations and apoptosis in the cells (Guo *et al.,* 2019); Resveratrol inhibited the EMT in CRC cells (Li *et al.,* 2019), etc., but there is still a long way to go and must continue to advance and deepen in order to reveal the anticancer mechanism of Chinese medicinal preparations and improve their clinical significance and economic value.

Atractylenolide I (ATL-I), a sesquiterpene molecule derived from the root of the traditional Chinese medicine *Atractylodes macrocephala*, is neuroprotective, antiallergic and anti-inflammatory, and suppresses tumor growth (Liu *et al.,* 2013; Qiao & Tian, 2022; Suzumiya *et al.,* 2009; H. Xu *et al.,* 2023). Some researches have found that ATL-I suppresses the growth of lung adenocarcinoma cells A549 nude mice transplantation tumors by activating the mitochondria-mediated apoptosis pathway (Liu *et al.,* 2013), as well as the proliferation of gastric cancer stem cells by blocking the Notch signaling system (Ma *et al.,* 2014). ATL-I overcame oxidative stress-induced malfunction in colonic mucosal epithelial cells (R. Xu *et al.,* 2023) and demonstrated anti-tumor activity in human CRC cells via the mitochondrial pathway (Chan *et al.,* 2020). Keratins are cellular intermediate filament proteins that regulate electrolyte transport in colonocytes, contribute to cell differentiation and proliferation and may play a role in inflammatory

**Corresponding authors:* e-mails: tongyo49510@163.com

signaling (Majumdar *et al.,* 2012; Polari *et al.,* 2020; J. Wu *et al.,* 2021). The expression of Keratin 7 (KRT7), a alkaline type II keratin, is associated with CRC tumor aggressiveness and survival duration (Bayrak *et al.,* 2012; Fei *et al.,* 2019; Loupakis *et al.,* 2019). Therefore, it is postulated that the inhibitory action of ATL-1 on CRC could be related with the down regulation of KRT7.

Intracellular signaling is a complicated regulation process that involves multiple pathways, links, and levels, such as energy metabolism in those, which runs throughout the cell and is a critical process for maintaining normal cellular life functions (Pentimalli *et al.,* 2019). Glucose is the main source of energy for cells and understanding its metabolism is vital for cell proliferation, growth and survival, as well as tumor progression (Zhu & Thompson, 2019). Maintaining glucose homeostasis is a critical physiological process regulated by hormones. The routine metabolism of glucose in cells mainly includes anaerobic glycolysis (the process of breaking down glucose to produce lactic acid under anaerobic conditions) and aerobic tricarboxylic acid cycle (Zhu *et al.,* 2022), however, the energy metabolism of cancer cells differs from that of normal cells and produces the Warburg effect, which means that under aerobic conditions, the cancer cells also metabolize glucose to lactate rather than pyruvate in this behavior (aerobic glycolysis) (Liberti & Locasale, 2016; Reinfeld *et al.,* 2022; Wang & Patti, 2023), which helps the cancer cells to better compete for resources in the nutrient-limited (Chang *et al.,* 2015; Liberti & Locasale, 2016). The identification of the aerobic glycolysis regulatory pathway is critical for understanding the processes of immune escape and treatment resistance in CRC cells.

In this investigation, we found that ATL-I reduced CRC cell proliferation and invasion and induced apoptosis. ATL-I also inhibited KRT7 expression and glycolysis. Furthermore, KRT7 expression was essential for ATL-I-induced reductions in cell proliferation, invasion and glycolysis, as well as apoptosis increased. Overall, our findings demonstrated a novel channel for ATL-I to exert anti-CRC activity, which may point in a new direction for the development of novel CRC medicines.

MATERIALS AND METHODS

Bioinformatics analysis

The KRT7 expression levels in colon adenocarcinoma (COAD) and rectal adenocarcinoma (READ) were predicted employing the GEPIA database (http://gepia.cancer-pku.cn/).

Cell lines and cultures

Human normal colon cells NCM460 and CRC cell lines (LoVo and HCT-116) were obtained from the Cell Center of the Shanghai Academy of Biological Sciences, Chinese Academy of Sciences. Cells were grown in RPIM-1640 medium (ORCPM0110B, ORiCells Biotechnology, Shanghai, China), which contained 10% fetal bovine serum (FBS). The cell lines were cultivated in a cell culture incubator at a constant temperature of 37°C with 5% CO_2. The number and condition of the cells were examined using a light microscope and cell passaging was performed when the density of adherent cells was greater than 80%.

Cell transfection

Ribobio (Guangzhou, China) provided the knockdown KRT7 (sh-KRT7) and negative control (sh-NC), as well as the overexpression KRT7 and negative control vector. The aforesaid vectors were then transfected into HCT-116 cells according to the Lipofectamine 3000 (L3000001, Invitrogen, Austin, TX, USA) instructions and the cells were grown in the incubator for 48 h.

Drug preparation

ATL-1 was acquired from MedChem Express (HY-N0201, Monmouth Junction, NJ, USA) and dissolved in 100 mM stock solution with dimethyl sulfoxide (ST1276, Beyotime, Shanghai, China). Before each experiment, the stock solution was diluted to the concentration specified in the experimental design.

qRT-PCR detection

Total RNA was isolated from all cell lines employing the TRIzol kit (DP424, TIANGEN, Beijing, China).RNA reverse transcription was carried out with the Prime Script RT Reagent Kit (RR047 A, Takara, Tokyo, Japan). The qRT-PCR assay was carried out using an ABI PRISM 7300 RT-PCR system (7300, ABI, Carlsbad, CA, USA) with the SYBR Green PCR kit (4309155, Applied Biosystems, Delaware, USA). The $2^{-\Delta\Delta Ct}$ technique was used to quantify the relative expression level of KRT7 mRNA, with β-actin serving as an internal reference. The primers were designed as follows (5′-3′): KRT7: F: 5'-TGTGGTGCTGAAGAAGGATGT-3'; R: 5'-TTCATCA CAGAGATATTCACGGCT-3'. β-actin: F: 5'-ATCACTA TTGGCAACGAGCG-3'; R: 5'-ACTCATCGTACTCCT GCTTG-3'.

Western blot analysis

Trypsin (T4799, Sigma-Aldrich, St. Louis, MO, USA) was used to digest isolated cells and protein was extracted by centrifugation after lysing the cells on ice in RIPA lysate (20101ES60, Yeasen, Shanghai, China). The concentration of protein in the supernatant was ascertained with a BCA kit (catalog number P0012, from Beyotime). Subsequently, the protein samples were applied to a 10% SDS-PAGE gel for separation, with a load of 20μg per lane. Post-electrophoresis, the proteins were transferred onto a PVDF membrane, which was then pre-treated with a 5% solution of BSA for one hour at ambient temperature to prevent undesired protein interactions and then rabbit anti-KRT7 (1:25, ab183344, Abcam, Waltham, MA, USA) and β-actin (1:1,000,

ab8227, Abcam) primary antibodies were added and incubated at 4ºC overnight. After TBST washing, sheep anti-rabbit IgG (1:2000, ab6721, Abcam) was added and incubated at room temperature for 30 min. TBST was washed and observed with ECL (P0018S, Beyotime) utilizing a 5200 visualizer (Tanon, Shanghai, China). The gray scale values of each protein band were quantitatively evaluated with Image J 1.8.0 (National Institutes of Health, Bethesda, MD, USA).

MTT cell proliferation assay

The MTT test was used to determine the influence of KRT7 expression level on the viability of HCT-116 cells, with three replicate wells set up in each group. HCT-116 cells in logarithmic growth phase were injected into 96-well plates. According to the directions for MTT reagent (ST316, Beyotime), MTT solution was added to HCT-116 cells and incubated, after which the medium was removed and dimethyl sulfoxide (ST1276, Beyotime) added to each well. The proliferative vitality of HCT-116 cells was assessed by measuring absorbance at 490 nm with an enzyme-labeled instrument.

Transwell cell invasion assay

Transwell determined the invasive potential of HCT-116 cells. Transwell chambers were inserted in 24-well plates. 50μL of Matrigel matrix gel (354234, Corning) was pre-filled and air-dried at room temperature for 4h. Cell culture solution (1×10^4 cells/well) and RPMI-1640 medium with 10% FBS were added to the wells beneath the chambers. The cell cultures were maintained at a temperature of 37ºC in an incubator with a 5% CO_2 atmosphere for a duration of 24 hours. Following this, the plates were taken out and the cellular material was preserved using a 4% paraformaldehyde solution for a period of 30 minutes. After fixation, the cells were subjected to staining with a 0.1% solution of crystal violet (C0121, Beyotime) for another 30 minutes. The cells were washed twice with PBS and dried and the quantity of cells invading the lower chamber was counted and photographed with a high magnification microscope (DM1000 Leica, Wetzlar, Germany).

Apoptosis detection with flow cytometry

After various treatments, HCT-116 cells were collected and inoculated on cell culture dishes at 1×10^5 cells/mL. Cells were stained with PI and Annexin V-FITC staining solution for 15 min at room temperature, following the directions on the PI/Annexin V-FITC kit (40302ES20, Yeasen). After adding 400μL of binding buffer, the staining was detected with a Novo Cyte Advanteon flow cytometer (Agilent Technologies, Santa Clara, CA, USA) and analyzed using Flow Jo v 10.6.2 (Tree Star Inc. Ashland, OR) software.

Kit measures glucose uptake, lactate and ATP generation levels

The levels of glucose absorption, lactate and ATP generation were detected using colorimetric methods by diluting the standards and samples according to the kit instructions. The kits contained a glucose uptake colorimetric kit (S0201S, Beyotime), a lactate colorimetric kit (D799851-0050, Sangon, Shanghai, China), and an ATP kit. A Spark multipurpose microplate reader (Tecan, Männedorf, ZH, Switzerland) was used to measure cell absorbance (glucose and lactate tests) and chemiluminescence intensity (ATP assay).

Animal experimentation

Model Organisms (Shanghai, China) provided eight five-week-old male BALB/c nude mice, which were then randomly divided into two groups of four mice each (Control and ATL-I). Mice were housed in a light/dark cycle treatment setting with a temperature of 22-26ºC, relative humidity of 50-60% and a 12-hour cycle. The mice were kept on a light/dark cycle. To create a tumor xenograft model, 1.5×10^6 cells of the transfected HCT-116 cell suspension were implanted into the right axilla of nude mice. After 5 days of feeding, mice in the ATL-I group received ALT-I (75mg/kg/d) via gavage, while mice in the Control group received saline. Every 5 days, the tumor volume (V) of mice was estimated using the formula $V=1/2\times L\times W^2$, where L represents the tumor's length and W represents its width. The mice were held for 25 days before being murdered, after which the tumors were meticulously isolated, weighed and photographed.

STATISTICAL ANALYSIS

Data from the experiments were analyzed using SPSS 26.0 software (SPSS Inc., Chicago, IL, USA) and presented as mean ± standard deviation. The *t*-test and ANOVA one-way analysis of variance measured differences between different groups. **P*<0.05 indicates statistically significant differences.

ETHICAL APPROVAL

This study was approved by Nanchong Key Laboratory of Individualized Drug Therapy (Grant No. NZ-20221023-A).

RESULTS

KRT7 is abundantly expressed in the CRC

We first predicted the expression level of KRT7 in CRC using the GEPIA website, which revealed that KRT7 was considerably elevated in both the COAD and READ databases (fig. 1A). The outcomes of qRT-PCR and Western blot analysis also showed that KRT7 expression was up-regulated in CRC cells (LoVo and HCT-116), and KRT7 expression was higher in HCT-116 cells compared to LoVo cells (fig. 1B-1D), hence the following investigations were performed using HCT-116 cells.

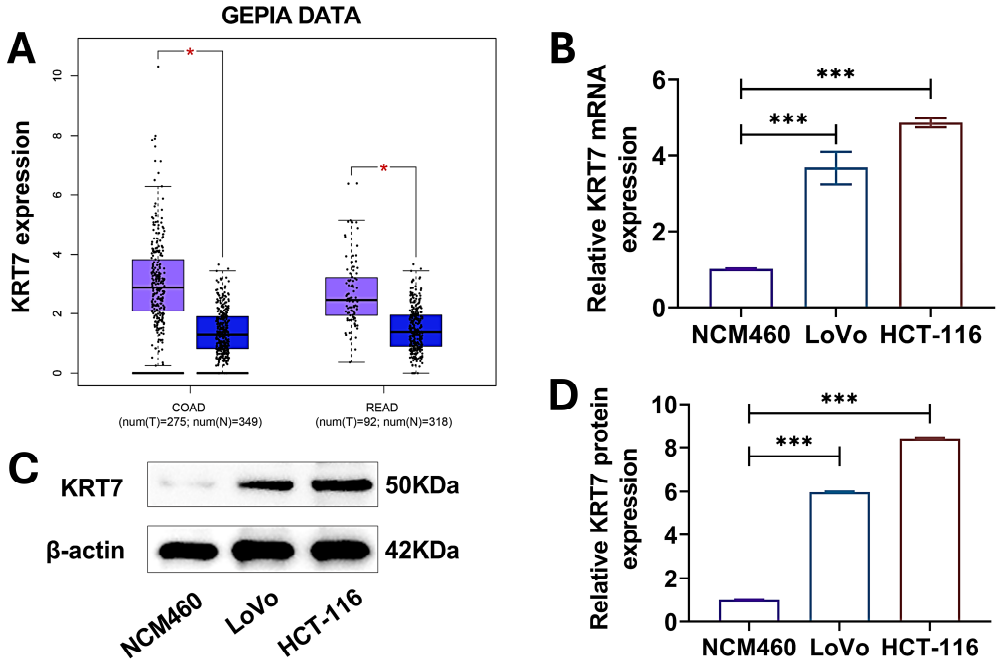

Fig. 1: KRT7 expression is upregulated in CRC
A The KRT7 expression levels in COAD and READ were predicted using the GEPIA online database.
B The mRNA levels of KRT7 in normal colon cells (NCM460) and CRC cell lines (LoVo, HCT-116) were determined using qRT-PCR.
C-D The level of KRT7 protein in normal colon cells (NCM460) and CRC cells (LoVo, HCT-116) was investigated using Western blot.

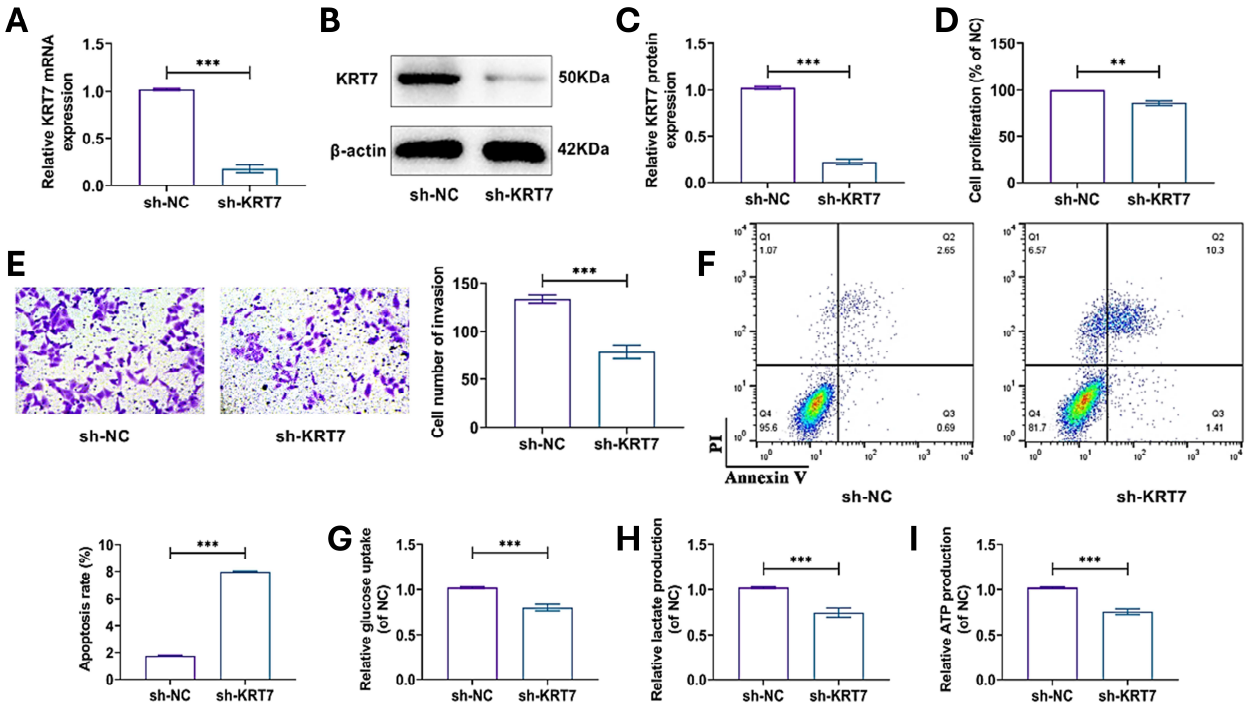

Fig. 2: Knocking down KRT7 reduces malignant biological processes and glycolysis in CRC cells.
A-C HCT-116 cells were transfected with sh-KRT7 and sh-NC, respectively. After 48 H of culture, the knockdown efficiency of KRT7 was validated using qRT-PCR and a Western blot assay.
D The effect of KRT7 knockdown on the proliferation of HCT-116 cells was determined using the MTT test.
E The amount of HCT-116 cells entering the bottom chamber following KRT7 knockdown was discovered using the Transwell assay.
F The impact of KRT7 knockdown on HCT-116 cell apoptosis was examined by flow cytometry to identify PI/Annexin V-FITC staining.
G-I Changes in glucose uptake, lactate and ATP generation in HCT-116 cells following KRT7 knockdown were measured using a kit.

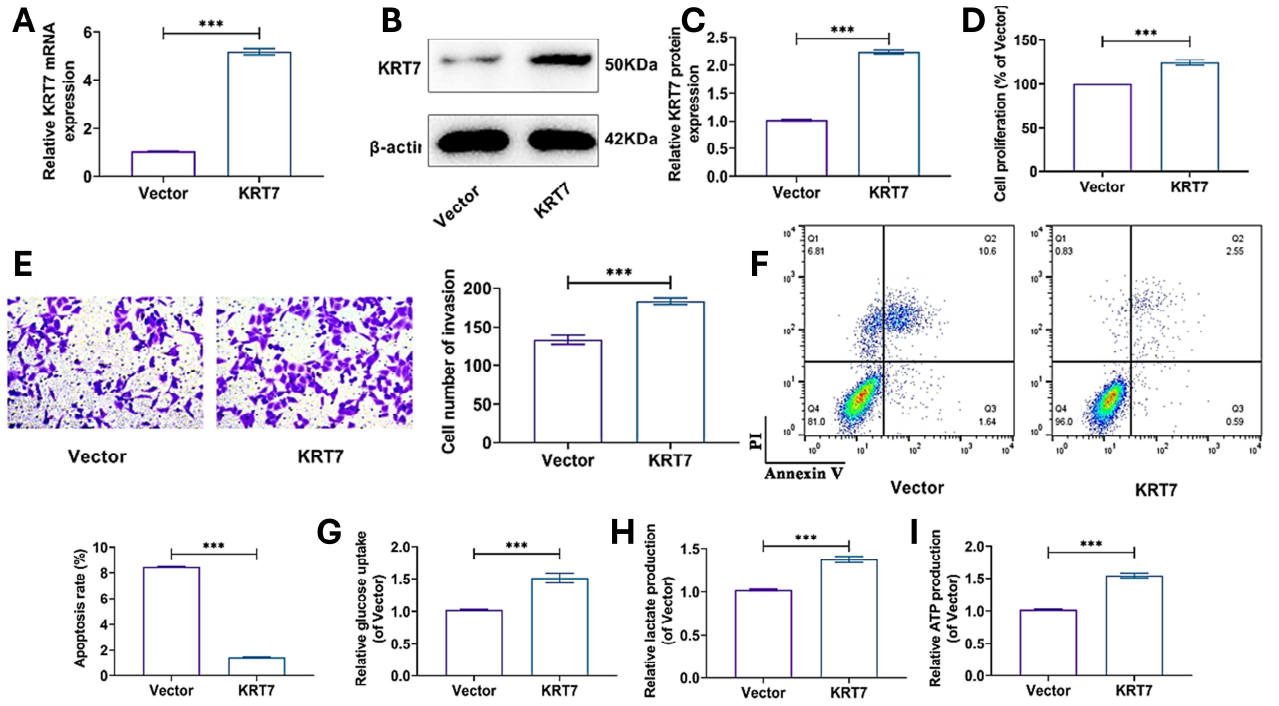

Fig. 3: Over expressing KRT7 suppresses carcinogenic biological processes and glycolysis in CRC cells

A-C Vector and KRT7 vectors were transfected into HCT-116 cells, and the over expression efficiency of KRT7 was determined using qRT-PCR and Western blot.
D The impact of KRT7 over expression on HCT-116 cell proliferation was evaluated using the MTT test.
E The number of HCT-116 cells invading the bottom chamber following KRT7 over expression was measured employing the Transwell assay.
F The impact of KRT7 overexpression on HCT-116 cell apoptosis was investigated by flow cytometry to identify PI/Annexin V-FITC staining.
G-I Changes in glucose uptake, lactate and ATP generation in HCT-116 cells following KRT7 over expression were measured using a kit.

Knockdown of KRT7 decreases CRC cell proliferation, invasion and glycolysis while promoting apoptosis

To identify KRT7's specific role in CRC, we used the sh-KRT7 interference vector and the over expression vector to down-regulate and up-regulate KRT7 expression in HCT-116 cells, respectively and then assessed the biological process and glycolytic alterations in HCT-116 cells.

The findings of qRT-PCR and Western blot assays demonstrated that transfection with sh-KRT7 vector dramatically lowered KRT7 levels in HCT-116 cells (fig. 2A-2C). MTT and Transwell assays revealed that reduction of KRT7 greatly reduced the proliferation rate and number of invasions of HCT-116 cells (fig. 2D-2E). The flow assay and quantitative analysis revealed that KRT7 down-regulation dramatically enhanced the death rate of HCT-116 cells (fig. 2F), resulting in a significant decrease in the glycolysis-related parameters glucose intake, lactate and ATP generation (fig. 2G-2I). The above laboratory results suggested that suppression of KRT7 decreased HCT-116 cell proliferation, invasion, and glycolysis while promoting cell apoptosis.

Over expression of KRT7 increases CRC cell proliferation, invasion and glycolysis while inhibiting apoptosis

Meanwhile, we transfected the KRT7 over expression vector into HCT-116 cells and confirmed that KRT7 mRNA and protein expression levels were successfully increased (fig. 3A-3C). In contrast to KRT7 knockdown, KRT7 over expression in HCT-116 cells increased cell proliferative viability (fig. 3D), boosted invasive ability (fig. 3E), and decreased apoptosis (fig. 3F). In addition, glucose consumption, lactate and ATP production were all significantly elevated with the upregulation of KRT7 (fig. 3G-3I). This shows that over expression of KRT7 increased proliferation, invasion and glycolysis while inhibiting apoptosis in HCT-116 cells, which could be the primary mechanism by which KRT7 promotes CRC development.

ATL-I suppresses CRC cell proliferation, invasion and glycolysis while promoting apoptosis

ATL-I has been shown to alter CRC cell apoptosis, glucose metabolism and stemness maintaining capacity, as well as inhibiting cell proliferation (Li *et al.* 2020). ATL-I is a sesquiterpene derived from the roots of Atractylodes macrocephala, with a chemical structure illustrated in fig. 4A and the molecular formula $C_{15}H_{18}O_2$. We treated HCT-116 cells with 0μM, 50μM, 100μM, 150μM and 200μM of ATL-I, respectively. The MTT assay revealed a significant difference in cell proliferation ability at a concentration of 150μM of ATL-I compared

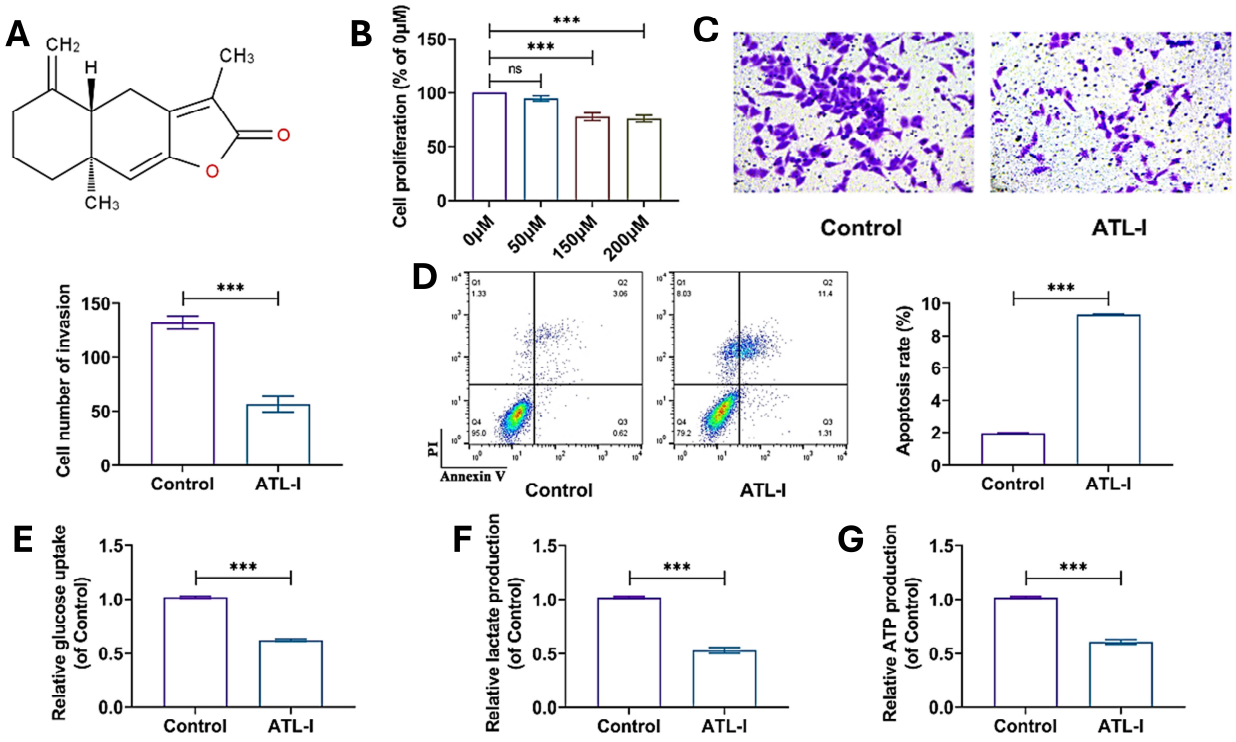

Fig. 4: ATL-I inhibits malignant biological processes and glycolysis in CRC cells

A Molecular structure of ATL-I.

B HCT-116 cells were treated with 0, 50, 150 and 200μM ATL-1, and the effects on cell viability were measured using the MTT method. The screen optimal treatment concentration was 150μM.

C HCT-116 cells were treated with 150μM ATL-1 and their invasion ability was assessed using the Transwell test.

D Flow cytometry was used to assess apoptotic levels in HCT-116 cells treated with 150μM ATL-1.

E-G The kits were used to detect the effect of 150μM ATL-1 on glucose uptake, lactate, and ATP generation in HCT-116 cells.

with 0μM (fig. 4B), so the subsequent experiments were performed at a concentration of 150μM of ATL-I treatment (the Control group used saline to treat the cells). The Transwell versus cell flow assay revealed that 150μM ATL-I treatment reduced HCT-116 cell invasiveness and dramatically enhanced apoptosis rate (fig. 4C-4D). Furthermore, 150μM ATL-I treatment reduced glycolysis in HCT-116 cells, resulting in lower glucose consumption, lactate and ATP generation levels (fig. 4E-4G). The results showed that 150μM ATL-I substantially inhibited the malignant biological behavior and glycolysis of CRC cells, while also promoting apoptosis.

KRT7 partially reverses ATL-I suppression of CRC cell proliferation, invasion, glycolysis and inhibits apoptosis

To further understand the relationship between KRT7 and ATL-I, we performed rescue assays in HCT-116 cells. Treatment with 150μM ALT-I dramatically reduced the protein expression of the KRT7 gene in HCT-116 cells (see fig. 5A). After that, we separated the trials into three groups: Control + Vector-NC (saline therapy + KRT7 empty vector treatment), ALT-I + Vector-NC (150 μM ALT-I+KRT7 empty vector treatment), and ALT-I + Vector-KRT7 (150μM ALT-I+KRT7 over expression vector treatment). After MTT, Trans well, flow cytometry experiments and relevant kit assays, we found that compared with the Control + Vector-NC group, cell proliferation viability, invasion and glycolysis levels were significantly down-regulated and apoptosis rate was significantly increased in the ALT-I + Vector-NC group, while over expression of the KRT7 gene effectively weakened the effect of ALT-I on HCT-116 cells, resulting in the re-enhancement of cell proliferation, invasion and glycolysis and a decrease in apoptosis rate (fig. 5B-5G). It was shown that ATL-I negatively regulates KRT7, and over expression of KRT7 significantly reversed ATL-I's inhibitory and apoptosis-promoting effects on the malignant biological behaviors of CRC cells.

Mice xenograft tumor test

To assess the cancer inhibiting impact of ATL-I *in vivo*, we injected HCT-116 cells subcutaneously into the right axilla of mice to create an *in vivo* CRC tumor model. Using a vernier caliper, the dimensions of the tumors, namely their length and width, were recorded, which allowed for the calculation of the tumor volume. After 15 days of upbringing, tumor growth in mice administered ATL-I was dramatically suppressed (fig. 6A). On the 25th day of feeding, the tumors in the ATL-I administration group were significantly smaller than those in the saline

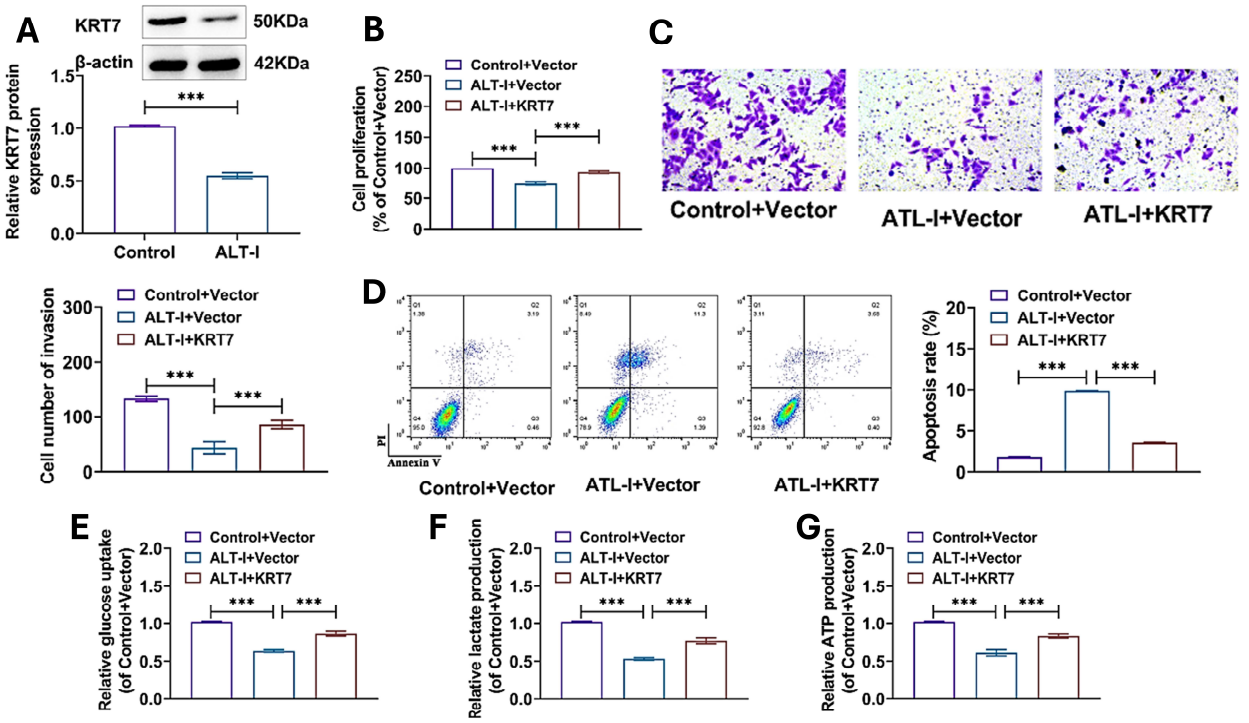

Fig. 5: KRT7 partially reversed ATL-I suppression of malignant biological processes and glycolysis in CRC cells

A Western blot analysis identified KRT7 protein level in HCT-116 cells treated with 150 μM ALT-I.
B The MTT test was used to investigate the effect of KRT7 expression on ATL-I-induced inhibition of HCT-116 cell proliferation.
C The Transwell assay was performed to determine the influence of KRT7 expression level on ATL-I in reducing HCT-116 cell invasion.
D The effect of KRT7 expression level on ATL-I-induced apoptosis in HCT-116 cells was measured by flow cytometry.
E-G The kits assessed the impact of KRT7 expression level on ATL-I inhibition of glucose uptake, lactate and ATP generation in HCT-116 cells.

control group (fig. 6B), and the weight of the tumors in the ATL-I administration group was found to be less than half that of the control group by weighing (fig. 6C). The study showed that ATL-I could successfully prevent tumor growth *in vivo*.

DISCUSSION

Chinese herbs' high efficacy, low toxicity, and side effects make them highly favorable and potentially useful in clinical cancer treatment, and they have become a research hotspot for various types of tumor immunotherapy (Nie *et al.,* 2016). In this work, we explored the regulatory effects of ATL-I, an active component of Atractylodes macrocephala, on the proliferation, invasion, apoptosis and glycolytic behaviors of CRC cells in order to demonstrate its inhibitory effects on CRC and understand its molecular processes. First, we discovered a large rise in the abundance of KRT7 in CRC patients using the GEPIA website. Furthermore, KRT7, a pro-oncogenic factor in CRC, responded partially to ATL-I's inhibitory effect on the malignant biological process of HCT-116 cells and was adversely regulated by ATL-I. As a result, we postulated that ATL-I exerts its anti-CRC effects by inhibiting KRT7 and that these effects are related to the suppression of the aerobic glycolytic pathway.

KRT7 is abnormally over expressed in malignant tumors including pancreatic cancer, bladder cancer, ovarian cancer, and CRC (An *et al.,* 2021; Czapiewski *et al.,* 2016; He *et al.,* 2021; Li *et al.,* 2021; Loupakis *et al.,* 2019; Yahyazadeh *et al.,* 2021; Zhang *et al.,* 2020). High KRT7 levels are strongly related with a bad prognosis, and KRT7 has been widely employed as a diagnostic and prognostic biomarker for a variety of cancers (Koren *et al.,* 2015; Li *et al.,* 2021; Y. Wu *et al.,* 2021). KRT7 has been shown to be expressed in approximately 10% of CRC tumors and is associated with increased tumor budding and a poor prognosis, it has the ability to enhance CRC cell metastasis (Chen *et al.,* 2020; Harbaum *et al.,* 2011). Another study discovered that KRT7 can promote aerobic glycolysis. Wu et al. (Wu *et al.,* 2022) discovered that primaquine might activate the EGFR/Akt glucose metabolism signaling pathway by targeting KRT7, enhancing aerobic glycolysis and reducing diabetes complications. Our experiment revealed that KRT7 expression was up-regulated in CRC cells, which could explain why CRC tumors grow malignantly and patients have a poor prognosis. Furthermore, over expression of KRT7 increased glucose consumption, lactate and ATP production in the cells, promoted the glycolytic pathway in HCT-116 cells and resulted in increased cell proliferation and invasion, implying that KRT7 is a

Fig. 6: Experiment *in vivo*

Mice were subcutaneously injected with HCT-116 cells to create an *in vivo* CRC tumor model. After 5 days of raising, mice in the ATL-I group were given ALT-I via gavage, while mice in the Control group received an identical volume of saline gavage. The volume of subcutaneous tumors was measured every 5 days with vernier calipers.
B-C Mice were killed on the 25th day of feeding, and the tumors were isolated, photographed, and weighed.

crucial component in the malignant development of CRC cells through glycolysis.

One of the most common characteristics in tumor cells is elevated aerobic glycolysis activation, which is known as a cancer hallmark (Hanahan & Weinberg, 2011). Cancer cells' metabolism is largely dependent on glycolysis and even under normal oxygen concentrations and fully functional mitochondrial conditions, most cancer cells produce energy via glycolysis, with the glycolytic pathway accounting for approximately 50% of adenosine triphosphate (ATP), also known as the Warburg effect or aerobic glycolysis (Bhattacharya *et al.,* 2016). This metabolic alteration causes larger amounts of lactic acid in the tumor microenvironment, resulting in tumor acidosis, which aids cancer cell adaption to hypoxic circumstances and promotes tumor development and invasiveness (Andreucci *et al.,* 2020). Inhibition of the glycolytic pathway can greatly reduce tumor cell invasion and limit cell growth and metastasis (Chen *et al.,* 2021; Fan *et al.,* 2021; Spencer & Stanton, 2019), hence finding effective glycolysis inhibitors is critical for treating CRC. Our experimental results demonstrated that 150μM of ALT-I efficiently lowered the amounts of glucose consumption, lactate, and ATP production in HCT-116 cells. This suggests that ATL-I can dramatically suppress glycolysis in CRC cells, which is consistent with prior findings (Li *et al.,* 2020). The study found that ATL-I has the potential to be a new CRC treatment agent. Furthermore, given that KRT7 can partially reverse to ATL-I's inhibitory effect on the malignant biological process of HCT-116 cells and is negatively regulated by ATL-I, it is reasonable to assume that ATL-I can inhibit the cellular glycolysis pathway by down-regulating KRT7 expression, weakening CRC cells' proliferative and invasive ability and inhibiting tumor growth.

CONCLUSION

Based on the findings, ATL-I suppressed the development of CRC cells in *vitro* and *in vivo*, and its anticancer characteristics may be attributed to the blockage of CRC cells' glycolytic pathway, which is influenced by the down-regulation of the ATL-I-regulated KRT7 gene. As a result, ATL-I inhibits the cellular glycolysis process primarily by down-regulating KRT7 expression, thus weakening the proliferation and invasion ability of CRC cells and inhibiting the growth of CRC tumors. The findings of this research could give a theoretical foundation for the development of future CRC drugs. Furthermore, ATL-I Chinese medicine preparation can be added to clinical chemotherapeutic medications to boost CRC drug sensitivity, regulate patients' immunity, and improve patients' prognosis.

REFERENCES

Aldea M, Andre F, Marabelle A, Dogan S, Barlesi F and Soria JC (2021). Overcoming resistance to tumor-targeted and immune-targeted therapies. *Cancer Discov.,* **11**(4): 874-899.

An Q, Liu T, Wang MY, Yang YJ, Zhang ZD, Liu ZJ and Yang B (2021). KRT7 promotes epithelial-mesenchymal transition in ovarian cancer via the TGF-beta/Smad2/3 signaling pathway. *Oncol. Rep.,* **45**(2): 481-492.

Andreucci E, Peppicelli S, Ruzzolini J, Bianchini F, Biagioni A, Papucci L, Magnelli L, Mazzanti B, Stecca B and Calorini L (2020). The acidic tumor microenvironment drives a stem-like phenotype in melanoma cells. *J. Mol. Med. (Berl.),* **98**(10): 1431-1446.

Bayrak R, Haltas H and Yenidunya S (2012). The value of CDX2 and cytokeratins 7 and 20 expression in differentiating colorectal adenocarcinomas from extraintestinal gastrointestinal adenocarcinomas: Cytokeratin 7-/20+ phenotype is more specific than CDX2 antibody. *Diagn. Pathol.,* **7**: 9.

Bhattacharya B, Mohd Omar MF and Soong R (2016). The Warburg effect and drug resistance. *Br. J. Pharmacol.,* **173**(6): 970-979.

Calibasi-Kocal G, Pakdemirli A, Bayrak S, Ozupek NM, Sever T, Basbinar Y, Ellidokuz H and Yigitbasi T (2019). Curcumin effects on cell proliferation, angiogenesis and metastasis in colorectal cancer. *J. Buon.,* **24**(4): 1482-1487.

Chan KWK, Chung HY and Ho WS (2020). Anti-tumor activity of Atractylenolide I in human colon adenocarcinoma *in vitro*. *Molecules,* **25**(1): 212.

Chang CH, Qiu J, O'Sullivan D, Buck MD, Noguchi T, Curtis JD, Chen Q, Gindin M, Gubin MM, van der Windt GJ, Tonc E, Schreiber RD, Pearce EJ and Pearce EL (2015). Metabolic competition in the tumor microenvironment is a driver of cancer progression. *Cell,* **162**(6): 1229-1241.

Chen JF, Wu SW, Shi ZM and Hu B (2023). Traditional Chinese medicine for colorectal cancer treatment: Potential targets and mechanisms of action. *Chin. Med.,* **18**(1): 14.

Chen S, Su T, Zhang Y, Lee A, He J, Ge Q, Wang L, Si J, Zhuo W and Wang L (2020). *Fusobacterium nucleatum* promotes colorectal cancer metastasis by modulating KRT7-AS/KRT7. *Gut Microbes,* **11**(3): 511-525.

Chen X, Hao B, Li D, Reiter RJ, Bai Y, Abay B, Chen G, Lin S, Zheng T, Ren Y, Xu X, Li M and Fan L (2021). Melatonin inhibits lung cancer development by reversing the Warburg effect via stimulating the SIRT3/PDH axis. *J Pineal Res.,* **71**(2): e12755.

Czapiewski P, Bobowicz M, Peksa R, Skrzypski M, Gorczynski A, Szczepanska-Michalska K, Korwat A, Jankowski M, Zegarski W, Szulgo-Paczkowska A, Polec T, Piatek M, Skokowski J, Haybaeck J, Zaczek A and Biernat W (2016). Keratin 7 expression in lymph node metastases but not in the primary tumour correlates with distant metastases and poor prognosis in colon carcinoma. *Pol. J. Pathol.,* **67**(3): 228-234.

El-Shami K, Oeffinger KC, Erb NL, Willis A, Bretsch JK, Pratt-Chapman ML, Cannady RS, Wong SL, Rose J, Barbour AL, Stein KD, Sharpe KB, Brooks DD and Cowens-Alvarado RL (2015). American Cancer Society Colorectal Cancer Survivorship Care Guidelines. *CA Cancer J. Clin.,* **65**(6): 428-455.

Fan Y, Wang J, Xu Y, Wang Y, Song T, Liang X, Jin F and Su D (2021). Anti-warburg effect by targeting HRD1-PFKP pathway may inhibit breast cancer progression. *Cell Commun. Signal,* **19**(1): 18.

Fei F, Li C, Cao Y, Liu K, Du J, Gu Y, Wang X, Li Y and Zhang S (2019). CK7 expression associates with the location, differentiation, lymph node metastasis, and the Dukes' stage of primary colorectal cancers. *J. Cancer,* **10**(11): 2510-2519.

Hanahan D and Weinberg RA (2011). Hallmarks of cancer: The next generation. *Cell,* **144**(5): 646-674.

Harbaum L, Pollheimer MJ, Kornprat P, Lindtner RA, Schlemmer A, Rehak P and Langner C (2011). Keratin 7 expression in colorectal cancer - freak of nature or significant finding? *Histopathology,* **59**(2): 225-34.

He Y, Yue H, Cheng Y, Ding Z, Xu Z, Lv C, Wang Z, Wang J, Yin C, Hao H and Chen C (2021). ALKBH5-mediated m(6)A demethylation of KCNK15-AS1 inhibits pancreatic cancer progression via regulating KCNK15 and PTEN/AKT signaling. *Cell Death Dis.,* **12**(12): 1121.

Koren A, Sodja E, Rijavec M, Jez M, Kovac V, Korosec P and Cufer T (2015). Prognostic value of cytokeratin-7 mRNA expression in peripheral whole blood of advanced lung adenocarcinoma patients. *Cell Oncol. (Dordr.),* **38**(5): 387-95.

Li Y, Su Z, Wei B and Liang Z (2021). KRT7 over-expression is associated with poor prognosis and immune cell infiltration in patients with pancreatic adenocarcinoma. *Int. J. Gen Med.,* **14**: 2677-2694.

Li Y, Wang Y, Liu Z, Guo X, Miao Z and Ma S (2020). Atractylenolide I induces apoptosis and suppresses glycolysis by blocking the JAK2/STAT3 signaling pathway in colorectal cancer cells. *Front Pharmacol.,* **11**: 273.

Liberti MV and Locasale JW (2016). The Warburg effect: How does it benefit cancer cells? *Trends Biochem. Sci.,* **41**(3): 211-218.

Liu H, Zhu Y, Zhang T, Zhao Z, Zhao Y, Cheng P, Li H, Gao H and Su X (2013). Anti-tumor effects of atractylenolide I isolated from *Atractylodes macrocephala* in human lung carcinoma cell lines. *Molecules,* **18**(11): 13357-13368.

Loupakis F, Biason P, Prete AA, Cremolini C, Pietrantonio F, Pella N, Dell'Aquila E, Sperti E, Zichi C, Intini R, Dadduzio V, Schirripa M, Bergamo F, Antoniotti C, Morano F, Cortiula F, De Maglio G, Rimassa L, Smiroldo V, Calvetti L, Aprile G, Salvatore L, Santini D, Munari G, Salmaso R, Guzzardo V, Mescoli C, Lonardi S, Rugge M, Zagonel V, Di Maio M and Fassan M (2019). CK7 and consensus molecular subtypes as major prognosticators in (V600E)BRAF mutated metastatic colorectal cancer. *Br. J. Cancer,* **121**(7): 593-599.

Ma L, Mao R, Shen K, Zheng Y, Li Y, Liu J and Ni L (2014). Atractylenolide I-mediated Notch pathway inhibition attenuates gastric cancer stem cell traits. *Biochem. Biophys. Res. Commun.,* **450**(1): 353-9.

Majumdar D, Tiernan JP, Lobo AJ, Evans CA and Corfe BM (2012). Keratins in colorectal epithelial function and disease. *Int. J. Exp. Pathol.,* **93**(5): 305-18.

Nie J, Zhao C, Deng LI, Chen J, Yu B, Wu X, Pang P and Chen X (2016). Efficacy of traditional Chinese medicine in treating cancer. *Biomed. Rep.,* **4**(1): 3-14.

Pachman DR, Qin R, Seisler DK, Smith EM, Beutler AS, Ta LE, Lafky JM, Wagner-Johnston ND, Ruddy KJ, Dakhil S, Staff NP, Grothey A and Loprinzi CL (2015). Clinical course of oxaliplatin-induced neuropathy: Results from the randomized phase III trial N08CB (Alliance). *J. Clin. Oncol.,* **33**(30): 3416-22.

Paleari L (2022). Cancer prevention with molecular targeted therapies. *Int. J. Mol. Sci.,* **23**(15).

Pentimalli F, Grelli S, Di Daniele N, Melino G and Amelio I (2019). Cell death pathologies: Targeting death pathways and the immune system for cancer therapy. *Genes Immun.,* **20**(7): 539-554.

Polari L, Alam CM, Nystrom JH, Heikkila T, Tayyab M, Baghestani S and Toivola DM (2020). Keratin intermediate filaments in the colon: Guardians of epithelial homeostasis. *Int. J. Biochem. Cell Biol.,* **129**: 105878.

Qiao P and Tian Z (2022). Atractylenolide I inhibits EMT and enhances the antitumor effect of cabozantinib in prostate cancer via targeting Hsp27. *Front Oncol,* **12**: 1084884.

Reinfeld BI, Rathmell WK, Kim TK and Rathmell JC (2022). The therapeutic implications of immuno-suppressive tumor aerobic glycolysis. *Cell Mol. Immunol.,* **19**(1): 46-58.

Spencer NY and Stanton RC (2019). The Warburg effect, lactate, and nearly a century of trying to cure cancer. *Semin Nephrol,* **39**(4): 380-393.

Sung H, Ferlay J, Siegel RL, Laversanne M, Soerjomataram I, Jemal A and Bray F (2021). Global Cancer Statistics 2020: GLOBOCAN estimates of incidence and mortality worldwide for 36 cancers in 185 Countries. *CA Cancer J. Clin.,* **71**(3): 209-249.

Suzumiya J, Ohshima K, Tamura K, Karube K, Uike N, Tobinai K, Gascoyne RD, Vose JM, Armitage JO, Weisenburger DD and International Peripheral TCLP (2009). The international prognostic index predicts outcome in aggressive adult T-cell leukemia/lymphoma: Analysis of 126 patients from the International Peripheral T-Cell Lymphoma Project. *Ann. Oncol.,* **20**(4): 715-21.

Wang H, Guan L, Li J, Lai M and Wen X (2018). The Effects of berberine on the gut microbiota in Apc (min/+) mice fed with a high fat diet. *Molecules,* **23**(9).

Wang Y and Patti GJ (2023). The Warburg effect: A signature of mitochondrial overload. *Trends Cell Biol.,* **33**(12): 1014-1020.

Wu J, Niu J, Li M and Miao Y (2021). Keratin 1 maintains the intestinal barrier in ulcerative colitis. *Genes Genomics,* **43**(12): 1389-1402.

Wu T, Li C, Zhou J, Han L, Qiang S, Hu Z, Liu J, Li X, Zhao W and Chen X (2022). Primaquine activates Keratin 7 to treat diabetes and its complications. *J. Diabetes Metab. Disord.,* **21**(2): 1731-1741.

Wu Y, Lv M, Qian T and Shen Y (2021). Correlation analysis of Ki67 and CK7 expression with clinical characteristics and prognosis of postoperative cervical adenocarcinoma patients. *Ann. Palliat. Med.,* **10**(9): 9544-9552.

Xu H, Li L, Qu L, Tu J, Sun X, Liu X and Xu K (2023). Atractylenolide-1 affects glycolysis/gluconeogenesis by downregulating the expression of TPI1 and GPI to inhibit the proliferation and invasion of human triple-negative breast cancer cells. *Phytother. Res.,* **37**(3): 820-833.

Xu R, Liu X Tian, M and Chen D (2023). Atractylodes-I overcomes the oxidative stress-induced colonic mucosal epithelial cells dysfunction to prevent irritable bowel syndrome via modulating the miR-34a-5p-LDHA signaling pathway. *Curr. Mol. Med.,* **23**(8): 825-833.

Yahyazadeh R, Bashash D, Ghaffari P, Kord S, Safaroghli-Azar A and Ghaffari, SH (2021). Evaluation of hTERT, KRT7, and survivin in urine for noninvasive detection of bladder cancer using real-time PCR. *BMC Urology,* **21**(1): 64.

Zhang Z, Tu K, Liu F, Liang M, Yu K, Wang Y, Luo Y, Yang B, Qin Y, He D, Jiang G, Huang O and Zou Y (2020). FoxM1 promotes the migration of ovarian cancer cell through KRT5 and KRT7. *Gene,* **757**: 144947.

Zhu J and Thompson CB (2019). Metabolic regulation of cell growth and proliferation. *Nat. Rev. Mol. Cell Biol.,* **20**(7): 436-450.

Zhu L, Zhu X and Wu Y (2022). Effects of glucose metabolism, lipid metabolism, and glutamine metabolism on tumor microenvironment and clinical implications. *Biomolecules,* **12**(4): 580.